AJO-DO

Numeric simulation model for long-term orthodontic tooth movement with contact boundary conditions using the finite element method

Ryo Hamanaka,[a] Satoshi Yamaoka,[a] Tuan Nguyen Anh,[a] Jun-ya Tominaga,[a] Yoshiyuki Koga,[b] and Noriaki Yoshida[a]
Nagasaki, Japan

Introduction: Although many attempts have been made to simulate orthodontic tooth movement using the finite element method, most were limited to analyses of the initial displacement in the periodontal ligament and were insufficient to evaluate the effect of orthodontic appliances on long-term tooth movement. Numeric simulation of long-term tooth movement was performed in some studies; however, neither the play between the brackets and archwire nor the interproximal contact forces were considered. The objectives of this study were to simulate long-term orthodontic tooth movement with the edgewise appliance by incorporating those contact conditions into the finite element model and to determine the force system when the space is closed with sliding mechanics. **Methods:** We constructed a 3-dimensional model of maxillary dentition with 0.022-in brackets and 0.019 × 0.025-in archwire. Forces of 100 cN simulating sliding mechanics were applied. The simulation was accomplished on the assumption that bone remodeling correlates with the initial tooth displacement. **Results:** This method could successfully represent the changes in the moment-to-force ratio: the tooth movement pattern during space closure. **Conclusions:** We developed a novel method that could simulate the long-term orthodontic tooth movement and accurately determine the force system in the course of time by incorporating contact boundary conditions into finite element analysis. It was also suggested that friction is progressively increased during space closure in sliding mechanics. (Am J Orthod Dentofacial Orthop 2017;152:601-12)

The prediction and planning of orthodontic tooth movement have largely depended on clinical experiences. If the long-term tooth movement can be accurately predicted, the treatment results will be greatly improved. With such a background, demand for simulating tooth movement under various loading conditions has been increasing in recent years. In orthodontic treatment, 2 phases of tooth movement are reiterated at each visit of a patient to the clinic. In the first phase, the application of orthodontic force induces the instantaneous deformation of the periodontal ligament (PDL), called "initial displacement." Then, in the second phase, the stress distributed in the PDL initiates bone remodeling. Thus, long-term orthodontic tooth movement occurs as a result of biomechanical and histologic changes in the periodontal tissues produced by the reiterations of the 2 phases consisting of mechanical and biologic processes.

Many finite element (FE) studies have been performed to simulate tooth movement to improve therapeutic efficiency in orthodontic treatment. Most were, however, limited to the analysis of initial displacement.[1-5] Although the initial displacement may be an indicator of the subsequent tooth movement after some bone remodeling, loading conditions change during tooth movement. In other words, as a tooth is tipped, the relationship between the line of action of the force and the location of the center of resistance (CR) of the tooth—the force system—is changing. It is therefore difficult to precisely predict overall tooth movement from the initial displacement. Incorporation of the bone remodeling process into the FE method is

[a]Department of Orthodontics and Dentofacial Orthopedics, Graduate School of Biomedical Sciences, Nagasaki University, Nagasaki, Japan.
[b]Department of Orthodontics, Nagasaki University Hospital, Nagasaki, Japan.
All authors have completed and submitted the ICMJE Form for Disclosure of Potential Conflicts of Interest, and none were reported.
Address correspondence to: Yoshiyuki Koga or Ryo Hamanaka, Department of Orthodontics and Dentofacial Orthopedics, Graduate School of Biomedical Sciences, Nagasaki University, 1-7-1 Sakamoto, Nagasaki 852-8588, Japan; e-mail, bb55313212@ms.nagasaki-u.ac.jp; koga@nagasaki-u.ac.jp.
Submitted, November 2016; revised and accepted, March 2017.
0889-5406/$36.00

http://dx.doi.org/10.1016/j.ajodo.2017.03.021

thus required to simulate the long-term tooth movement more accurately.

Only a few studies investigating bone remodeling with the FE method have been performed. Bourauel et al[6,7] and Schneider et al[8] simulated orthodontic tooth movement for a simplified single-root tooth using the FE method based on bone remodeling theories. In these simulations, alveolar bone geometries must be updated each time small amounts of bone remodeling are calculated; thus, such methods are time-consuming when trying to simulate the long-term movements of multiple teeth simultaneously. Kojima and Fukui[9-14] and Kojima et al[15-17] performed numeric analyses to simulate long-term tooth movements of multiple teeth by using special elements that represented teeth supported by PDLs in an FE model. In those studies, however, neither the play between the brackets and archwire nor the interproximal contact force was considered. A previous study showed that the play between the brackets and archwire has a large impact on the tooth movement pattern.[1] Moreover, the contact forces between teeth are thought to substantially affect the force system acting on the tooth and its resultant movement. To our knowledge, no previous study has considered both the bracket-wire interface and the interproximal contact force in the numeric analysis of orthodontic tooth movement. An analysis incorporating these 2 mechanical conditions will determine the force system in sliding mechanics, which has been mechanically indeterminate when using conventional methods.

The purposes of this study were to develop a method to simulate long-term orthodontic tooth movement with contact boundary conditions based on the FE method and to determine the force system acting on each tooth in sliding mechanics using a model with realistic bracket slot, archwire, and tooth dimensions. See Supplemental Materials for a short video presentation about this study.

MATERIAL AND METHODS

Three-dimensional (3D) images of a maxillary dentition were obtained from a dry skull using a multi-image microcomputed tomography scanner (3DX; J. Morita, Kyoto, Japan) with a voxel size of 80 μm. The data were exported as a DICOM file to 3D image processing and editing software (Mimics 10.02; Materialise, Leuven, Belgium). Then the DICOM data were reconstructed to 3D surface data and imported to FE analysis preprocessing and postprocessing software (Patran 2012.1; MSC Software, Los Angeles, Calif) as 3-node triangular elements. These triangular elements were converted to 4-node quadrilateral elements. After remeshing, the teeth were aligned to the ideal positions to make a normal dentition. Each interproximal space between adjacent teeth was set to be less than 0.01 mm.

The PDL was constructed on the root surface with 8-node hexahedral elements. The thickness was determined to be a uniform 0.2 mm,[18] because a previous study showed that whether the PDL is uniform or not does not make a significant difference in the strain distribution in the PDL.[19]

The coordinate system of the analysis model was defined so that the x-axis pointed in the transverse direction, the y-axis in the anteroposterior direction, and the z-axis in the vertical direction, with the positive direction to the left, posterior, and up, respectively (Fig 1). All analyses were performed using an FE package (Marc 2014.1; MSC Software).

The PDL was modeled as a nonlinear (bilinear) isotropic material. An elastic modulus from 0.03 to 0.3 MPa and a Poisson's ratio of 0.3 were assigned to the PDL according to previous studies.[20,21] To develop a more simplified model for reducing the analysis time, the tooth material was assumed to be a rigid body, since an orthodontic force is small, thereby causing only a small amount of tooth deformation, which can be negligible. Therefore, we modeled the teeth using thin shell elements with a thickness of 3.0 mm and a Young's modulus of 204 GPa, which is 10 times higher than the previously reported value.[22,23] A Poisson's ratio of 0.3 was also assigned. In a preliminary analysis, we verified that this tooth model had enough stiffness.

Figure 2 shows an algorithm for simulating long-term orthodontic tooth movement. As the first step, an orthodontic force is applied to the tooth model. Then the initial displacement is produced reflecting the deformed PDL. When we take measurements of the initial tooth displacement, the alveolar bone is assumed to be a rigid body, since its deformation is negligible compared with that of the PDL. According to this assumption, displacements are constrained at the outer surface of the PDL. This procedure omits the need to model the alveolar bone. Consequently, the analysis time for calculating bone deformation and remeshing the solid elements of the deformed alveolar bone, which had been done in previous studies, was eliminated.[7,8]

As the second step, each node forming the outer surface of the PDL is displaced so that the PDL is restored to its original configuration and thickness of 0.2 mm. In other words, the geometry of the PDL is updated on the assumption that the orthodontic tooth movement is correlated with the initial displacement, since that assumption has been accepted by the widely recognized theory of orthodontic mechanics.[24-26] Thus, the alveolar

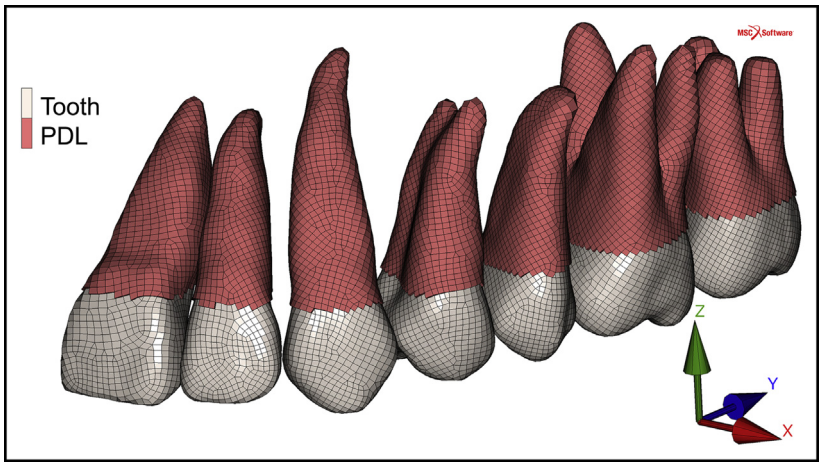

Fig 1. Three-dimensional FE model of maxillary dentition and coordination system.

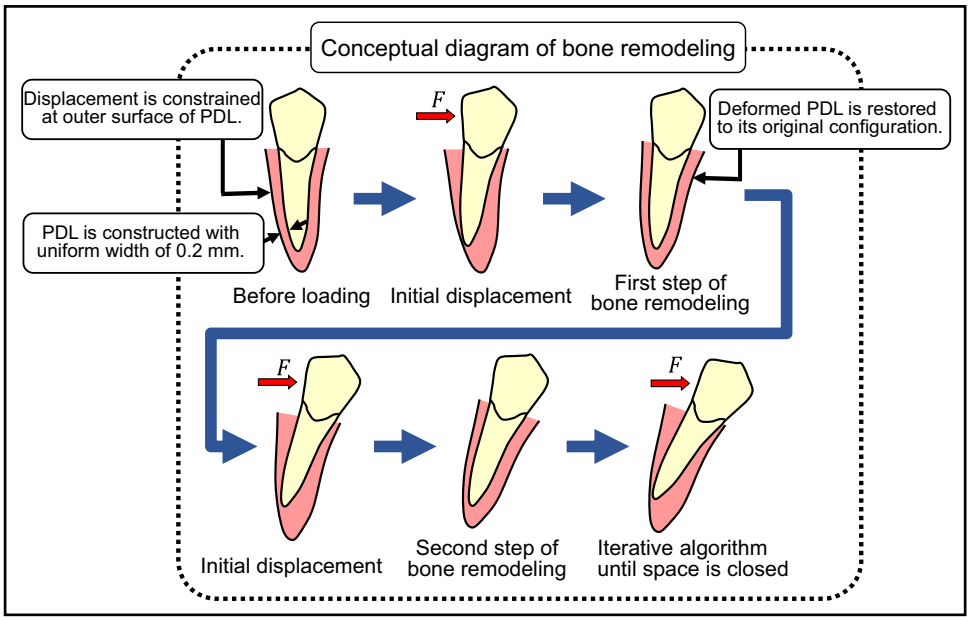

Fig 2. Diagram of an algorithm for simulating long-term tooth movement.

bone is remodeled so that the space between the tooth and the alveolus is kept constant during the long-term movement.[7] In this manner, the alveolar bone remodeling is simulated after the first application of an orthodontic force.

Subsequently, the second orthodontic force is applied to the tooth model. At this time, displacements are constrained to the outer surface of the PDL whose geometry is updated through the process of the first remodeling, and initial displacement is again produced. Then, these 2 steps—the initial displacement and bone remodeling—are iterated to simulate orthodontic tooth movement after the long-term process of absorption and apposition of the alveolar bone. These procedures are executed automatically using custom-developed subroutines.

Contact boundary conditions, which used the node-to-segment function of the Marc software, were applied to each interproximal surface of the tooth.[27] A contact surface was formed on the midsagittal plane for symmetric analysis (Fig 3).

The method for evaluating 3D tooth movement is described as follows. Three-dimensional motion can be described as a combination of translation and rotational

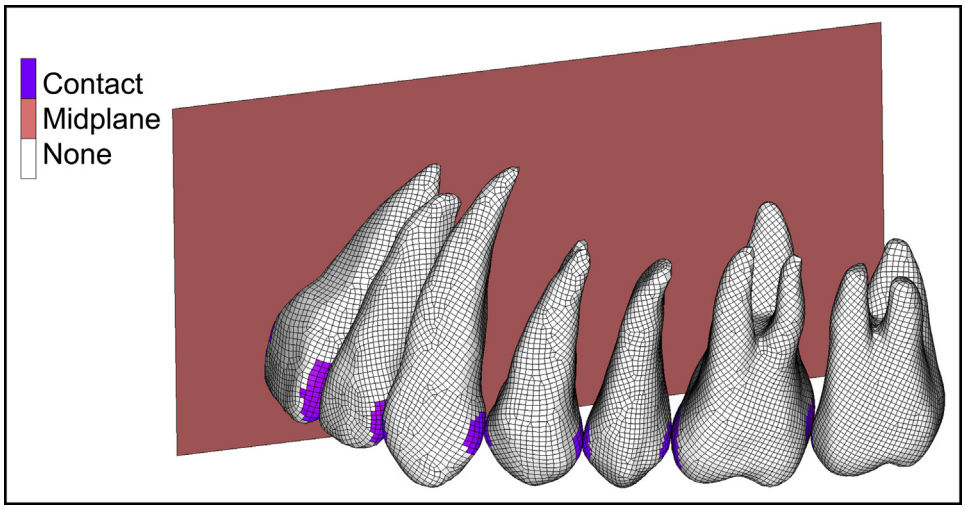

Fig 3. Contact boundary conditions on interproximal surfaces of teeth.

motion around an arbitrary point. The center of gravity is generally used as the center of rotation to describe motions in rigid body dynamics. Instead of the center of gravity, the CR is commonly applied in the mechanical theory of orthodontic tooth movement. Thus, the tooth movements were quantified by measuring the rotation of each tooth body and the translation of the CR. The rotation and translation were calculated from the entries of the transformation matrix between the initial position and the resulting position.[28,29] However, previous studies have shown that the CR does not exist as a point in 3D space, and the direction of the applied force that translates a tooth does not necessarily correspond to that of a moving CR because of the geometric asymmetry of a tooth.[30,31] Therefore, the CR is determined expediently using the following method (Fig 4).

1. Three arbitrary nodes on each tooth are chosen, and displacement boundary conditions are prescribed; ie, displacement U_i is assigned to each node in the distal direction. Let U_i be defined as $U_i = (L\sin\theta_i, L\cos\theta_i, 0)$, where L is 0.02 mm, and θ_i is the angle between U_i and the x-axis.
2. Each reaction force acting on the 3 nodes that are subjected to displacement is calculated.
3. A single counter force, which is balanced with a resultant force of the 3 force vectors, is determined. This force translates the tooth model in the U_i direction. We confirmed that the tooth moves bodily on applying the force to the model.
4. Another displacement $U_i^{'} = (L\sin(\theta_i+90^o), L\cos(\theta_i+90^o), 0)$ is assigned to the 3 nodes perpendicular to U_i in the transverse direction.
5. Each reaction force acting on the 3 nodes is calculated. Then, a single counter force that translates the tooth model in the $U_i^{'}$ direction is calculated in the same manner as 2 and 3.
6. The closest point between the lines of action of the 2 forces, which translate the tooth model in the U_i and $U_i^{'}$ directions, respectively, is calculated. Let CR_i (center of resistance) be the point determined.
7. Each position of CR_i is calculated on applying forces running in several different directions parallel to the occlusal plane, since it varies depending on the direction of U_i. The ultimate position of the CR of the tooth model is determined as the point in which each coordinate value of CR_i is averaged. Thus, the position of the CR is represented by the following equation: $CR = \sum_{i=1}^{360} CR_i/360$

The Table shows the determined positions of the CR for each tooth model.

An analysis of tooth movement during space closure using sliding mechanics was performed on the assumption that the case model was diagnosed as maxillary protrusion, and extraction of premolars was indicated. The first premolar and its PDL were removed from the model. The extraction space was set to be 4 mm, considering the consumption of space during the initial leveling.

An appliance consisting of 0.022 × 0.028-in slot passive self-ligating brackets and a 0.019 × 0.025-in stainless steel archwire was modeled (Fig 5). The front end of the archwire, on the midsagittal plane, was constrained in the x-direction for symmetric analysis. The Young's modulus and Poisson's ratio of the archwire and brackets were set to 204 GPa and 0.3, respectively. Contact boundary conditions were prescribed on the

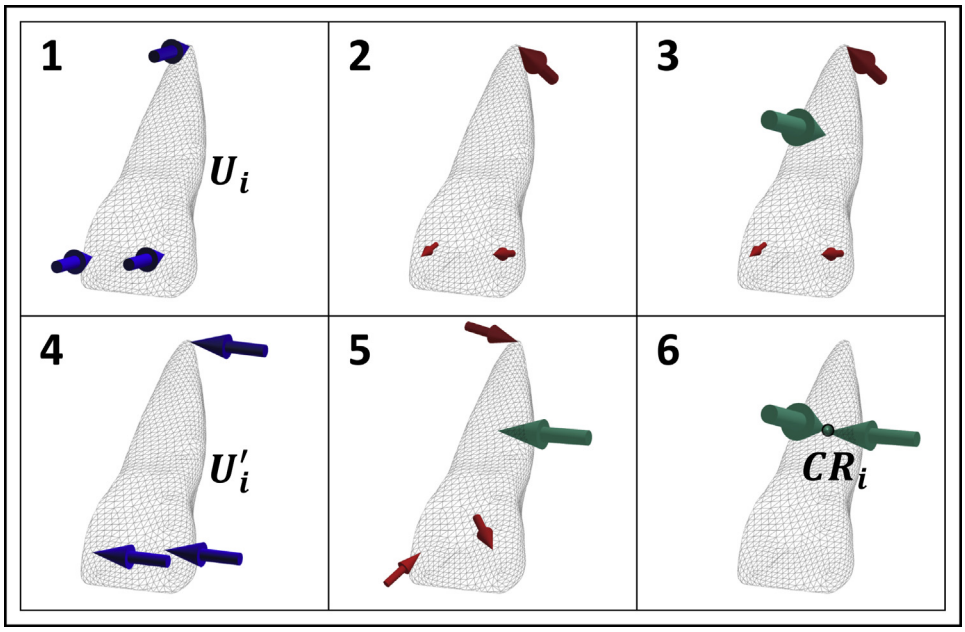

Fig 4. Method to determine the CR of a tooth. The *blue*, *red*, and *green arrows* represent the directions of displacement (U_i and U_i') and the reaction force acting on the 3 nodes and 1 counter force that translates the tooth, respectively. CR_i is the closest point between the lines of action of the 2 counter forces.

Table. Determined positions of CR for each tooth model

Maxillary tooth	*Distance to CR from bracket level (mm)*
Central incisor	7.1
Lateral incisor	7.7
Canine	9.0
First premolar	8.0
Second premolar	7.9
First molar	9.2
Second molar	7.6

surfaces of the archwire and brackets. To improve the accuracy of the contact analysis, the contact boundary surfaces were represented using a Coons patch. The bracket was connected to each tooth with truss elements. For space closure, a retraction force is applied to a node on the archwire corresponding to a midpoint between the lateral incisor and canine brackets, and a reaction force is applied at the mesial end of the second molar tube. The force magnitude was set to be 100 cN. The force vectors were updated on each remodeling procedure in the software to fit a new tooth position.

RESULTS

The extraction space was completely closed after the bone remodeling steps were iterated 121 times with the FE analysis software. Anterior and posterior teeth were tipped into the extraction site, and bowing occurred (Fig 6).

Based on the results of this analysis, an animated Video was created that shows how tooth movement proceeds from the initial displacement to the space closure (see Video, available at www.ajodo.org).

Figure 7 shows the relationship between the angle of rotation around the x-axis (lingual crown tipping) and the y-component of displacements of the CRs of the anterior teeth (translation). The horizontal axis shows the displacements of the CRs in the posterior direction, and the vertical axis indicates the degree of lingual crown tipping for the central and lateral incisors, and distal tipping for the canine. The degree of lingual crown tipping or distal tipping for each tooth significantly increased as its CR moved posteriorly. When the extraction space was closed, the displacements of the CR were found to be 0.9, 0.9, and 1.5 mm for the central incisor, lateral incisor, and canine, respectively, and the degrees of rotation were 14.1°, 13.8°, and 9.0°, respectively. The degree of rotation increased constantly throughout space closure. Although the degree of distal tipping of the canine increased at the beginning in the same manner as the central incisor or lateral incisor, the rate of increase in the degree of rotation gradually decreased.

Figure 8 shows the normal contact force generated at the interface between the brackets and archwire. The

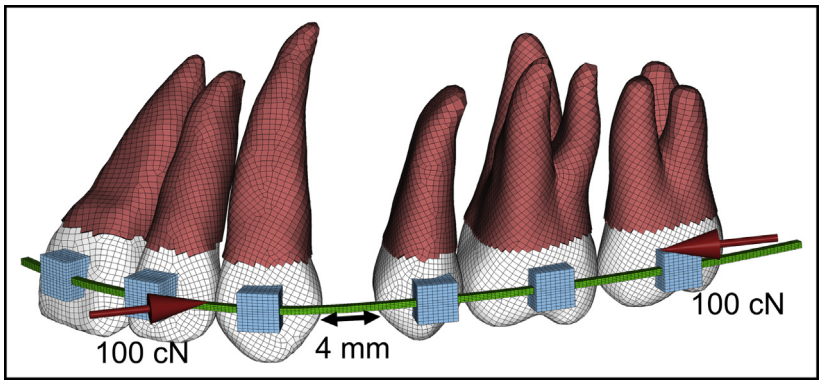

Fig 5. Model equipped with sliding mechanics. The red arrows represent the retraction force. The extraction space was set at 4 mm.

arrows represent the direction and magnitude of the normal contact force exerted on the corners of the brackets by the archwire. At the initial displacement step (remodeling = 0), the normal contact force between the archwire and brackets was generated only at the bottom surface of the brackets of the anterior teeth, and no normal contact force was generated at the brackets of the posterior teeth. After the bone remodeling was iterated more than 10 times, the normal contact force was produced also at the second premolar and the first molar in the vertical direction and at the second molar in the horizontal direction. The magnitude of normal contact force acting on the posterior teeth increased throughout space closure.

Antitipping moments generated at the interface between the brackets and archwire in the sagittal plane were calculated from the normal contact force vectors. Figure 9 shows the moment-to-force (M/F) ratios transmitted to the brackets from the archwire as a function of the number of bone remodeling steps. The value of M/F ratio smaller than the distance from the bracket to the CR indicates lingual crown tipping for the central incisor and lateral incisor, and distal tipping for the canine. The M/F ratios transmitted to the central incisor, lateral incisor, and the canine reached maximum values of 1.1, 7.0, and 21.8 mm, respectively.

Figure 10 shows the normal contact force vectors generated at interproximal contact points between adjacent teeth. The arrows represent the direction and magnitude of the normal contact force exerted on a contact point of each tooth against its adjacent tooth. Although normal contact forces were generated on the posterior teeth, no contact force was produced on the anterior teeth at the initial displacement step (remodeling = 0). After the bone remodeling was iterated several times, contact forces were distributed to the anterior teeth as well as the posterior teeth.

The magnitude of the moment generated by the contact force was calculated in the same way as the moment exerted on the tooth by the archwire. Figure 11 shows the M/F ratios transmitted to the brackets from both the archwire and adjacent teeth. At step 121 of the bone remodeling, the M/Fs transmitted to the central incisor, lateral incisor, and canine were 5.1, 7.9, and 9.3 mm, respectively.

DISCUSSION

Although many studies have been performed to predict orthodontic tooth movement, most were limited to the analysis of initial displacement,[1-5,32,33] which was mainly produced from physical distortion of the PDL, thus making the movement momentary and reversible. On the other hand, orthodontic tooth movement is observed as a result of histologic changes in periodontal tissues adjacent to a tooth after the long-term process of bone or tissue remodeling. Bourauel et al[7] simulated long-term movement of a single tooth using the FE method on the assumption that bone remodeling is controlled predominantly by the strain rather than the stress. Kojima and Fukui[9-14] and Kojima et al[15-17] performed numeric analyses of orthodontic tooth movement for an entire dentition. However, simulating the long-term movement of multiple teeth simultaneously is time-consuming, and neither the play between the brackets and archwire nor the interproximal contact force was considered in their FE analyses.

To accurately simulate the long-term orthodontic movement of multiple teeth, a number of issues must be overcome. First, the analysis time should be reduced,

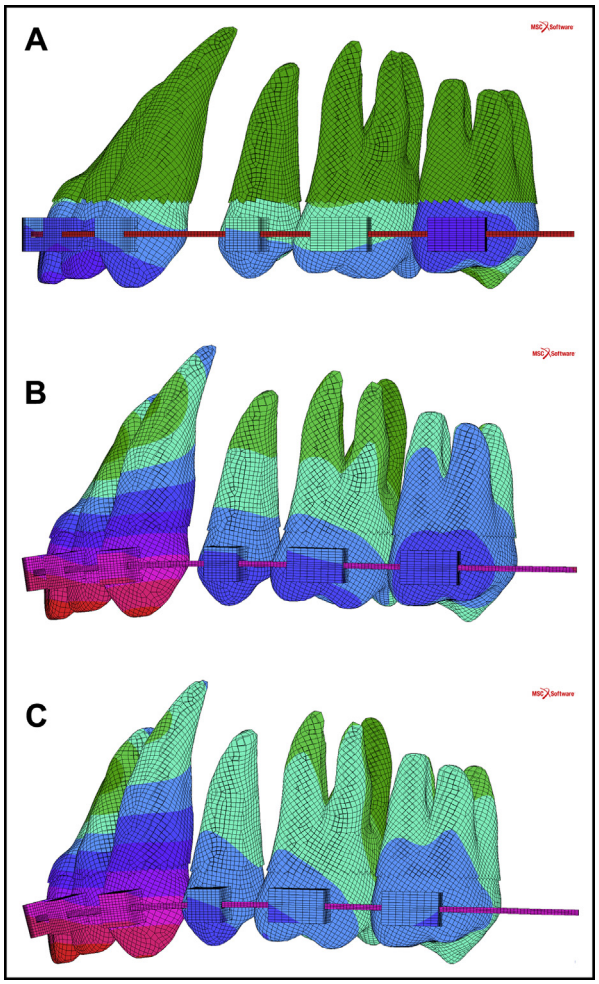

Fig 6. Tooth displacement during space closure: **A,** initial displacement; **B,** displacement at the midpoint of space closure (at the 60th bone remodeling step); **C,** displacement at the end of space closure (at the 121st bone remodeling step).

since the analysis of a model composed of an enormous number of solid elements including tooth, PDL, and alveolar bone takes a long time. Second, the contact boundary conditions must be taken into account in the FE model.

To reduce the number of elements, thereby minimizing the analysis time, the FE model was simplified. We used shell elements instead of solid elements for the tooth model. Our preceding analysis showed that the analysis using solid elements was too time-consuming because of the nonlinearity of the contact analysis. Moreover, the modeling of the alveolar bone was omitted by constraining the displacement of the outer surface of the PDL. The displacement boundary condition was updated over and over again instead of

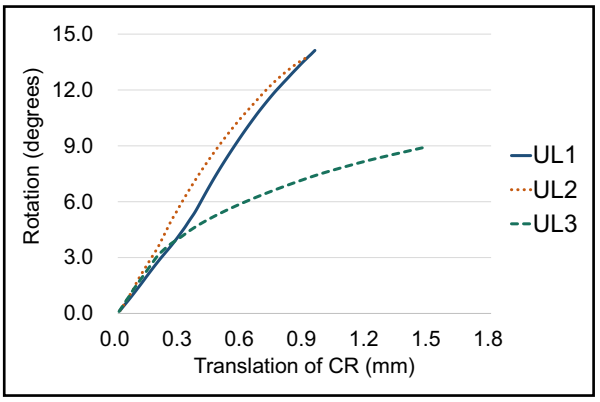

Fig 7. Degree of tooth rotation around the x-axis as a function of translation of the CR in the y-axis direction. *Positive signs* indicate lingual crown tipping; *negative signs* indicate lingual root tipping.

modifying alveolar bone elements at each step. These steps were performed on the assumption that the alveolar bone is a rigid body, since its deformation is negligible compared with that of the PDL. In this manner, simplification of the model could substantially reduce the analysis time. The bone remodeling process was required to be iterated 121 times until the extraction space was completely closed in our analysis. Such an enormous amounts of calculations cannot be done without simplification of the model.

This analysis suggested that contact boundary conditions not only on the interface between the bracket and archwire but also on the interproximal contact points between adjacent teeth should be incorporated into the FE model. In the preliminary study, we found that the surfaces of canine and incisors were overlapped if the interproximal contact with the adjacent teeth was not considered. In addition, the play between the archwire and brackets also made a difference in the tooth movement pattern. To construct the actual clinical situation, a 0.019 × 0.025-in stainless steel archwire and 0.022 × 0.028-in slot brackets with contact boundary conditions were modeled in this analysis. As a result, the degree of lingual crown tipping of the central incisor was determined to be 14.1°, which was significantly greater than the value obtained in a previous study.[11] It was probably because neither the play between the brackets and archwire nor the interproximal contact force was considered in that study. The discrepancy between the results of these studies could indicate that constructing realistic models and incorporating contact boundary conditions into the interface between the bracket and archwire and between the adjacent teeth are essential to accurately simulate orthodontic tooth movement.

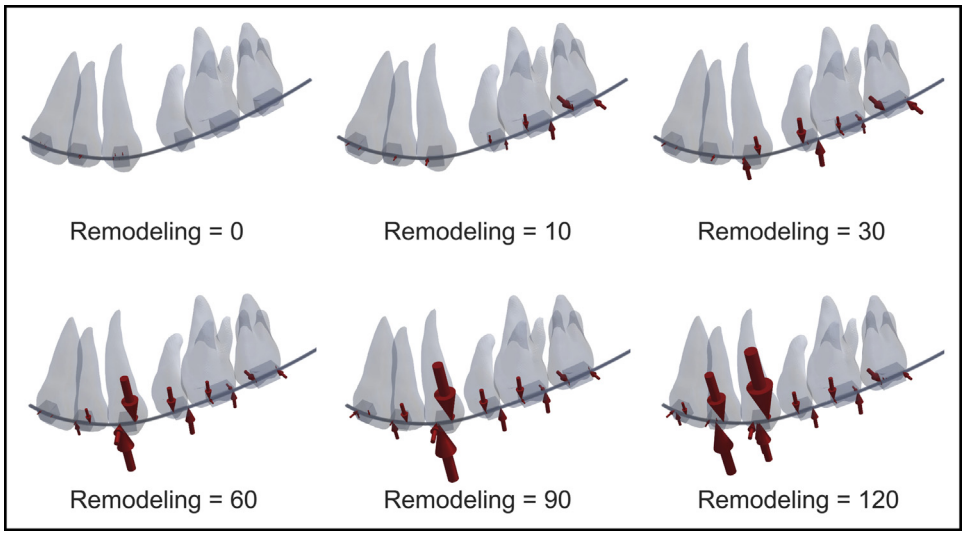

Fig 8. Normal contact force generated at the interface between the brackets and archwire. *Arrows* represent the vector of the normal contact force exerted on the corners of the brackets by the archwire. The larger arrow indicates larger force.

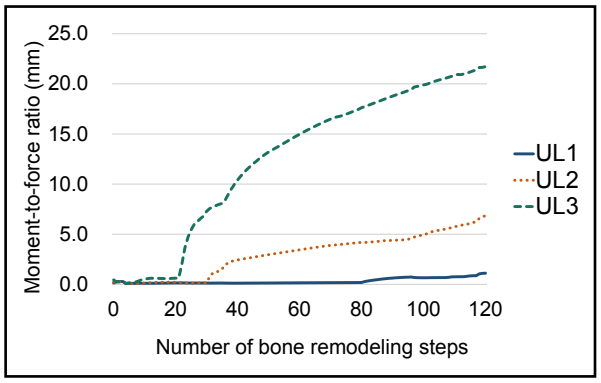

Fig 9. The M/F ratios transmitted to the brackets from the archwire as a function of the number of bone remodeling steps.

Tooth movement as rigid-body motion can be described as a combination of translation and rotational motion around an axis of rotation that is fixed in the tooth, such as the CR.[34] Previous studies have suggested that the CR is the most suitable reference point for expressing tooth movement, since a pure moment does not displace it, and force passing through it does not generate rotation.[24-26] Therefore, the degree of rotation was plotted as a function of the amount of translation for describing the movement pattern of the anterior teeth in Figure 7.

The incisors and canine showed different tipping patterns and displacement amounts. The displacement amounts of the incisors were significantly smaller than that of the canine, and the incisors tipped more than did the canine, although the line of action of the retraction force was common among the anterior teeth. These results suggested that the movement pattern of a tooth cannot be simply predicted from the relationship between the line of action of a force and the location of the CR in the edgewise appliance.

In a clinical situation, the anterior teeth should be moved bodily in the posterior direction after finishing the initial leveling stage and obtaining the optimal inclination. When bodily movement is achieved, displacements of the CRs must be the same among the anterior teeth. However, the amount of displacement for the incisors was significantly smaller than that of the canine. Displacement amounts of the CRs were 0.9 mm for central and lateral incisors and 1.5 mm for the canine; these are extremely small compared with the extraction space of 4 mm after leveling. From a clinical perspective, when the bowing effect is produced during space closure as an undesirable side effect, a lingual root tipping moment should be applied to obtain the proper inclination for each incisor. Simultaneously, the incisors' CRs should be distalized more substantially than the canine's CR, since a greater displacement of the CR to the final position at the treatment goal is required for the incisors than for the canine.

The M/F ratio transmitted from the archwire is approximately zero at the beginning of space closure (Fig 9). Then, the M/F ratios increase rapidly for the canine and gradually for the lateral incisor from the 20th and 30th steps of bone remodeling, respectively.

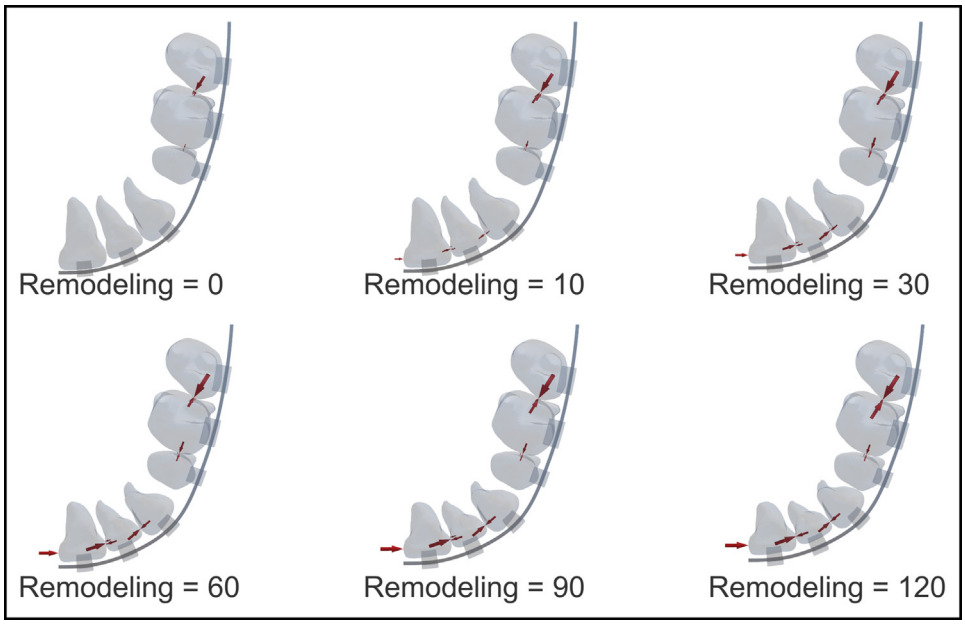

Fig 10. Normal contact force generated at interproximal contact points between adjacent teeth. *Arrows* represent the vector of the normal contact force exerted on a contact point of each tooth against its adjacent tooth.

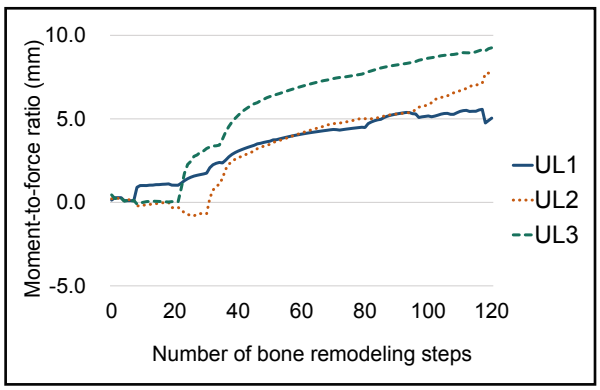

Fig 11. The M/F ratios transmitted to the brackets from both the archwire and adjacent teeth as a function of the number of bone remodeling steps.

However, the M/F ratio acting on the central incisor remains at zero for the greater part of space closure and is increased from the 80th step of bone remodeling up to the maximum value of only 1.1 mm. When the M/F ratio is lower than the distance to the CR from the point of force application (bracket position), the central and lateral incisors are subjected to lingual crown tipping moments, and the canine to a distal tipping moment. Conversely, when the M/F ratio is greater than the distance to the CR from the point of force application, each tooth tips in the opposite direction. The M/F ratio transmitted from the archwire to the central and lateral incisors reached maximum values of 1.1 and 7.0 mm, respectively. Each value of those M/F ratios is smaller than the distance to the CR from the bracket levels of 7.1 mm for the central incisor and 7.7 mm for the lateral incisor. Therefore, both incisors are considered to be subjected to lingual crown tipping moments; consequently, our analysis showed the same results. However, there was no significant difference in the degree of tipping between the 2 incisors in spite of the big difference in the M/F ratio (Fig 7; Table). On the other hand, the M/F ratio acting on the canine exceeded 9.0 mm, which is the distance to the CR from the bracket position, and reached the maximum value of 21.8 mm. Such a high M/F ratio is likely to cause the canine to tip medially. Nevertheless, this analysis gave the opposite results. These contradictions seem to be caused by the contact force acting at the interproximal contact point between adjacent teeth.

The force system—the force and moment acting on each tooth—has 2 components. One is the force and moment transmitted from the archwire at the interface between the bracket and archwire, and the other is the force and moment transmitted from the adjacent tooth at the interproximal contact point.

The y-component of the force transmitted from the adjacent tooth is directed posteriorly for the canine (Fig 10). That is, the canine is subjected to the contact

force from the lateral incisor in the posterior direction. Thus, the forces transmitted from the archwire and from the adjacent tooth are added together in the posterior direction. As a result, the canine receives a greater distal force. At the same time, the overall antitipping moment is decreased due to the contact force transmitted from the lateral incisor in the posterior direction. Contrary to this, the central incisor is subjected to the contact force transmitted from the lateral incisor in the anterior direction. In other words, the force transmitted from the archwire in the posterior direction is partly cancelled by the force transmitted from the adjacent tooth. Consequently, the force acting on the central incisor becomes smaller compared with the force acting on the canine. The force acting on the lateral incisor also becomes smaller in the same manner as the central incisor. Thus, the central and lateral incisors are pushed forward by the contact force transmitted from the lateral incisor and canine, respectively. The forces exerted on both incisors in the posterior direction are decreased. The total antitipping moment acting on the central incisor is increased because of the contact force transmitted from the lateral incisor in the anterior direction.

Consequently, the total M/F ratios, with those transmitted from both the archwire and adjacent teeth are added together, were 5.1 mm for the central incisor, 7.9 mm for the lateral incisor, and 9.3 mm for the canine at the end of space closure (Fig 11). The similarity of the tipping between the central and lateral incisors, and the distal tipping of the canine, can be explained well by these values of the total M/F ratios. The value of the total M/F ratio is remarkably higher for the central incisor and less than half for the canine in comparison with the M/F ratio transmitted from the archwire. If the tooth movement and force system are analyzed without considering the contact forces between the teeth, all analyses could be flawed. These results suggest that not only the contact between the brackets and archwire but also the contact between teeth must be taken into account to accurately determine the force system and to simulate the tooth movement in the edgewise appliance.

Our analysis shows that the magnitude and distribution of the normal contact force exerted on the corners of the brackets on the molars by the archwire changed dramatically during space closure (Fig 8). Since the amount of friction is represented by the product of the normal contact force and the coefficient of friction, generation of the normal contact force is critical in the posterior region. Although the normal contact forces are not generated on the posterior teeth during the early phase of space closure, they appear in the vertical direction on the second premolar and first molar from the 10th step of bone remodeling. The force progressively increases particularly on the first molar during space closure. In other words, increases in the friction on the second premolar and the first molar tend to prevent the archwire from sliding through the bracket and tubes on the posterior segment. This may explain why the rate of tooth movement is decreased in the latter phase of space closure in sliding mechanics.

The model developed in this study made it possible to evaluate the changes of M/F ratio and friction while the space is closed in sliding mechanics. The bracket prescription would make a difference in the amount of normal contact force generated at the interface between the bracket and archwire. For example, use of a conventional bracket ligated with an elastomeric ring is likely to increase contact forces and friction, which could substantially affect the tooth movement pattern and the rate of tooth movement. We can take advantage of this simulation model to investigate the effect of the bracket prescription and the method of ligation on orthodontic tooth movement. Similarly, we can compare the effects of treatment mechanics such as sliding and loop mechanics, different dimensions of archwire with respect to the size of bracket slot, buccal and lingual bracket systems, and so on only by replacing the materials in future analyses.

It should be verified whether the assumption that orthodontic tooth movement is correlated to initial tooth displacement is reliable. From the perspective of biomechanics, that assumption has been accepted by the widely recognized theory of orthodontic mechanics.[24-26] Many studies have been conducted to measure initial tooth displacement for the prediction of orthodontic tooth movement.[35-37] From the perspective of biologic study integrated with biomechanics, it was previously suggested that bone remodeling is related to stress or strain distribution in the periodontium.[38,39] As for bone apposition, Viecilli et al[40] reported the correlation between the maximum principal stress in the PDL and the amount of bone apposition under well-controlled mechanical and genetic conditions in mice. However, it is still unclear how much bone volume is resorbed under a specified stress or strain condition. Since the initial displacement is strongly correlated to the strain of the PDL, which induces biologic responses, we performed FE analyses based on the simple assumption that orthodontic tooth movement is correlated with the initial tooth displacement.

On the other hand, the material properties of the PDL change during orthodontic tooth movement. Also, the width of the PDL is not constant but increases as the tooth is moved. The effect of these changes on tooth movement certainly cannot be ignored. However, it has not been clarified how and to what extent the

morphologic and functional changes of the PDL affect overall tooth movement. Those factors should be incorporated into an FE model in the future study.

We are currently investigating the correlation between the strain or stress distributed in the PDL and the rate of bone remodeling, which is measured with 3D digital model analysis for human subjects. If these data are fed back to FE analyses, an exceedingly accurate simulation for long-term orthodontic tooth movement could be achieved.

CONCLUSIONS

We developed a time-dependent FE model that enables the prediction of orthodontic tooth movement. Long-term tooth movement could be successfully simulated by incorporating contact boundary conditions not only on the interface between the bracket and archwire but also on the interproximal contact points between adjacent teeth into the FE analysis. As a result, changes in the force system—the tooth movement pattern during space closure in sliding mechanics—could be accurately determined. The analysis showed that friction is progressively increased during space closure. This may prevent the archwire from sliding through the bracket and tubes on the posterior segment and decrease the rate of tooth movement in the latter phase of space closure in sliding mechanics.

SUPPLEMENTARY DATA

Supplementary data related to this article can be found at http://dx.doi.org/10.1016/j.ajodo.2017.03.021.

REFERENCES

1. Tominaga JY, Ozaki H, Chiang PC, Sumi M, Tanaka M, Koga Y, et al. Effect of bracket slot and archwire dimensions on anterior tooth movement during space closure in sliding mechanics: a 3-dimensional finite element study. Am J Orthod Dentofacial Orthop 2014;146:166-74.
2. Ozaki H, Tominaga JY, Hamanaka R, Sumi M, Chiang PC, Tanaka M, et al. Biomechanical aspects of segmented arch mechanics combined with power arm for controlled anterior tooth movement: a three-dimensional finite element study. J Dent Biomech 2015;6: 1758736014566337.
3. Kanjanaouthai A, Mahatumarat K, Techalertpaisarn P, Versluis A. Effect of the inclination of a maxillary central incisor on periodontal stress. Finite element analysis. Angle Orthod 2012;82: 812-9.
4. Nihara J, Gielo-Perczak K, Cardinal L, Saito I, Nanda R, Uribe F. Finite element analysis of mandibular molar protraction mechanics using miniscrews. Eur J Orthod 2015;37:95-100.
5. Liang W, Rong Q, Lin J, Xu B. Torque control of the maxillary incisors in lingual and labial orthodontics: a 3-dimensional finite element analysis. Am J Orthod Dentofacial Orthop 2009;135: 316-22.
6. Bourauel C, Vollmer D, Jäger A. Application of bone remodeling theories in the simulation of orthodontic tooth movements. J Orofac Orthop 2000;61:266-79.
7. Bourauel C, Freudenreich D, Vollmer D, Kobe D, Drescher D, Jäger A. Simulation of orthodontic tooth movements. A comparison of numerical models. J Orofac Orthop 1999;60:136-51.
8. Schneider J, Geiger M, Sander FG. Numerical experiments on long-time orthodontic tooth movement. Am J Orthod Dentofacial Orthop 2002;121:257-65.
9. Kojima Y, Fukui H. Numerical simulations of canine retraction with T-loop springs based on the updated moment-to-force ratio. Eur J Orthod 2012;34:10-8.
10. Kojima Y, Fukui H. Effects of transpalatal arch on molar movement produced by mesial force: a finite element simulation. Am J Orthod Dentofacial Orthop 2008;134:1-7.
11. Kojima Y, Fukui H. Numeric simulations of en-masse space closure with sliding mechanics. Am J Orthod Dentofacial Orthop 2010; 138:702.e1-6.
12. Kojima Y, Fukui H. Numerical simulation of canine retraction by sliding mechanics. Am J Orthod Dentofacial Orthop 2005;127: 542-51.
13. Kojima Y, Fukui H. A numerical simulation of tooth movement by wire bending. Am J Orthod Dentofacial Orthop 2006;130:452-9.
14. Kojima Y, Fukui H. A finite element simulation of initial movement, orthodontic movement, and the centre of resistance of the maxillary teeth connected with an archwire. Eur J Orthod 2014; 36:255-61.
15. Kojima Y, Fukui H, Miyajima K. The effects of friction and flexural rigidity of the archwire on canine movement in sliding mechanics: a numerical simulation with a 3-dimensional finite element method. Am J Orthod Dentofacial Orthop 2006;130:1-10.
16. Kojima Y, Mizuno T, Fukui H. A numerical simulation of tooth movement produced by molar uprighting spring. Am J Orthod Dentofacial Orthop 2007;132:630-8.
17. Kojima Y, Mizuno T, Umemura S, Fukui H. A numerical simulation of orthodontic tooth movement produced by a canine retraction spring. Dent Mater J 2007;26:561-7.
18. Tominaga JY, Tanaka M, Koga Y, Gonzales C, Kobayashi M, Yoshida N. Optimal loading conditions for controlled movement of anterior teeth in sliding mechanics. Angle Orthod 2009;79: 1102-7.
19. Hohmann A, Kober C, Young P, Dorow C, Geiger M, Boryor A, et al. Influence of different modeling strategies for the periodontal ligament on finite element simulation results. Am J Orthod Dentofacial Orthop 2011;139:775-83.
20. Papadopoulou K, Hasan I, Keilig L, Reimann S, Eliades T, Jäger A, et al. Biomechanical time dependency of the periodontal ligament: a combined experimental and numerical approach. Eur J Orthod 2013;35:811-8.
21. Papadopoulou K, Keilig L, Eliades T, Krause R, Jäger A, Bourauel C. The time-dependent biomechanical behaviour of the periodontal ligament—an in vitro experimental study in minipig mandibular two-rooted premolars. Eur J Orthod 2014;36:9-15.
22. Kinney JH, Balooch M, Marshall SJ, Marshall GW, Weihs TP. Hardness and Young's modulus of human peritubular and intertubular dentine. Arch Oral Biol 1996;41:9-13.
23. Meredith N, Sherriff M, Setchell DJ, Swanson SA. Measurement of the microhardness and young's modulus of human enamel and dentine using an indentation technique. Arch Oral Biol 1996;41: 539-45.
24. Burstone CJ. The biomechanics of tooth movement. In: Kraus BS, Riedel RA, editors. Vistas in orthodontics. Philadelphia: Lea & Febiger; 1963. p. 197-213.

25. Haack DC. The science of mechanics and its importance to analysis and research in the field of orthodontics. Am J Orthod 1963;49: 330-45.
26. Smith RJ, Burstone CJ. Mechanics of tooth movement. Am J Orthod 1984;85:294-307.
27. Carpenter NJ, Taylor RL, Katona MG. Lagrange constraints for transient finite element surface contact. Int J Numer Methods Eng 1991;32:103-28.
28. Horn BK. Closed-form solution of absolute orientation using unit quaternions. J Opt Soc Am A 1987;4:629.
29. Horn BK, Hilden HM, Negahdaripour S. Closed-form solution of absolute orientation using orthonormal matrices. J Opt Soc Am A 1988;5:1127.
30. Viecilli RF, Budiman A, Burstone CJ. Axes of resistance for tooth movement: does the center of resistance exist in 3-dimensional space? Am J Orthod Dentofacial Orthop 2013;143:163-72.
31. Dathe H, Nägerl H, Kubein-Meesenburg D. A caveat concerning center of resistance. J Dent Biomech 2013;4: 1758736013499770.
32. Yoshida N, Jost-Brinkmann PG, Koga Y, Mimaki N, Kobayashi K. Experimental evaluation of initial tooth displacement, center of resistance, and center of rotation under the influence of an orthodontic force. Am J Orthod Dentofacial Orthop 2001;120: 190-7.
33. Sia S, Shibazaki T, Koga Y, Yoshida N. Experimental determination of optimal force system required for control of anterior tooth movement in sliding mechanics. Am J Orthod Dentofacial Orthop 2009;135:36-41.
34. Kurashima K. Graphic solution of extraoral anchorage. J Japan Orthod Soc 1982;41:556-61.
35. Burstone CJ, Pryputniewicz RJ. Holographic determination of centers of rotation produced by orthodontic forces. Am J Orthod 1980;77:396-409.
36. Vanden Bulcke MM, Burstone CJ, Sachdeva RCL, Dermaut LR. Location of the centers of resistance for anterior teeth during retraction using the laser reflection technique. Am J Orthod Dentofacial Orthop 1987;91:375-84.
37. Pedersen E, Andersen K, Melsen B. Tooth displacement analysed on human autopsy material by means of a strain gauge technique. Eur J Orthod 1991;13:65-74.
38. Katona TR, Paydar NH, Akay HU, Roberts WE. Stress analysis of bone modeling response to rat molar orthodontics. J Biomech 1995;28:27-38.
39. Saito M, Saito S, Ngan PW, Shanfeld J, Davidovitch Z. Interleukin 1 beta and prostaglandin E are involved in the response of periodontal cells to mechanical stress in vivo and in vitro. Am J Orthod Dentofacial Orthop 1991;99:226-40.
40. Viecilli RF, Katona TR, Chen J, Hartsfield JK Jr, Roberts WE. Orthodontic mechanotransduction and the role of the P2X7 receptor. Am J Orthod Dentofacial Orthop 2009;135:694.e1-16: discussion, 694-5.